

Allylic Alkylations Catalyzed by Palladium Systems Containing Modular Chiral Dithioethers. A Structural Study of the Allylic Intermediates

Fernando Fernández,[†] Montserrat Gómez,^{*,†} Susanna Jansat,[†] Guillermo Muller,[†] Erika Martín,^{*,‡} Leticia Flores-Santos,[‡] Paula X. García,[‡] Alberto Acosta,[‡] Ali Aghmiz,[§] Marta Giménez-Pedros,[§] Anna M. Masdeu-Bultó,[§] Montserrat Diéguez,[§] Carmen Claver,[§] and Miguel Ángel Maestro[⊥]

Departament de Química Inorgànica, Universitat de Barcelona, Martí i Franquès 1-11, E-08028 Barcelona, Spain, Departamento de Química Inorgànica, Facultad de Química, Universidad Nacional Autónoma de México, Cd. Universitaria, 04510 México DF, México, Departament de Química Física i Inorgànica, Universitat Rovira i Virgili, c/ Marcel·lí Domingo, s/n, E-43007 Tarragona, Spain, and Edificio anexo Facultad de Ciencias, Servicios Xerais de Apoio á Investigación, Campus da Zapateira, s/n, Universidade da Coruña, E-15071 A Coruña, Spain

Received March 15, 2005

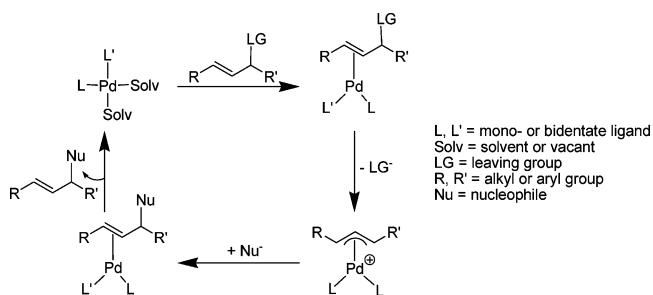
Palladium allylic systems containing modular chiral dithioether ligands were chosen as catalysts for a systematic study of homodonor ligands in allylic alkylation reactions. For this purpose, new type-DMPS (**4–6**) and -DEGUS (**8, 9**) ligands were synthesized. Dithioethers **4–6** afforded high activities and excellent selectivities in all Pd-catalyzed allylic reactions. Particularly the Pd/**6** catalytic system provided **b-VIII** with an ee > 99% and a regioselectivity **I/b (VIII)** = 1/1.6. A family of intermediate complexes containing several allyl groups (symmetrical, **13–16** and **20**, and nonsymmetrical, **17–19**, moieties) and dithioether ligands (**4–6, 8, 9, 11**, and **12**) is described. The complexes were fully characterized both in solution and in the solid state. X-ray structures of four of these complexes (**16–18** and **20**) were determined. The diastereomers present in solution were studied by NMR spectroscopy, and in some cases it was possible to establish a relationship between the diastereomeric excesses and the selectivities found in the catalytic process.

Introduction

The development of efficient methods for the enantioselective construction of carbon–carbon bonds is an ongoing central theme in organic synthesis research.¹ Among the C–C coupling reactions, metal-catalyzed asymmetric allylic alkylation allows the formation of new stereogenic C-centers.² In the accepted mechanism for this reaction with stabilized carbon nucleophiles and heteronucleophiles (Scheme 1), the enantioselective-determining step is the intermolecular nucleophilic attack on the terminal allylic carbons. To achieve high ee, these two carbon atoms must be differentiated and the dynamic behavior of the allylic coordinated moiety must be controlled via the $\eta^3\text{-}\eta^1\text{-}\eta^3$ mechanism.^{2c}

Heterodonating ligands such as P,S-,³ P,N-,⁴ and N,S-⁵ are effective inducers of enantioselectivity in this reaction due to the different *trans*-effect of the donor atoms. However, P,P-, N,N-, and S,S-homodonor ligands

Scheme 1. Mechanism Accepted for Pd-Catalyzed Allylic Substitutions with Soft Nucleophiles



have also provided high ee in this reaction.^{2,6} In this case, for those with C_2 -symmetry, the number of possible diastereomeric intermediates is reduced and the stereodifferentiation has been related to steric interactions. In fact, palladium complexes containing bis-(thioglycoside) ligands provided excellent enantioselectivity.

* Corresponding author. Fax: +33561558204. E-mail: gomez@chimie.ups-tlse.fr.

[†] Universitat de Barcelona.

[‡] Universidad Nacional Autónoma de México.

[§] Universitat Rovira i Virgili.

[⊥] Universidade da Coruña.

(1) Ojima, I. *Catalysis in Asymmetric Synthesis*, 2nd ed.; Wiley-VCH: New York, 2000.

(2) (a) Trost, B. M.; Crawley, M. L. *Chem. Rev.* **2003**, *103*, 2921. (b) Pfaltz, A. *Acc. Chem. Res.* **1993**, *26*, 339. (c) Gogoll, A.; Oernebros, J.; Grennberg, H.; Bäckvall, J.-E. *J. Am. Chem. Soc.* **1994**, *116*, 3631.

(3) (a) Evans, D. A.; Campos, K. R.; Tedrow, J. R.; Michael, F. E.; Gagné, M. R. *J. Org. Chem.* **1999**, *64*, 2994. (b) Albinati, A.; Pregosin, P. S.; Wick, K. *Organometallics* **1996**, *15*, 2419. (c) Enders, D.; Peters, R.; Lochtmann, R.; Raabe, G.; Runsink, J.; Bats, J. W. *Eur. J. Org. Chem.* **2000**, 3399. (d) Hiroi, K.; Suzuki, Y.; Abe, I. *Tetrahedron: Asymmetry* **1999**, *10*, 1173. (e) Pàmies, O.; van Strijdonck, G. P. F.; Diéguez, M.; Deerenberg, S.; Net, G.; Ruiz, A.; Claver, C.; Kamer, P. C. J.; van Leeuwen, P. W. N. M. *J. Org. Chem.* **2001**, *66*, 8867. (f) Selvakumar, K.; Valentini, M.; Pregosin, P. S. *Organometallics* **1999**, *18*, 4591. (g) Evans, D. A.; Campos, K. R.; Tedrow, J. R.; Michael, F. E.; Gagné, M. R. *J. Am. Chem. Soc.* **2000**, *122*, 7905.

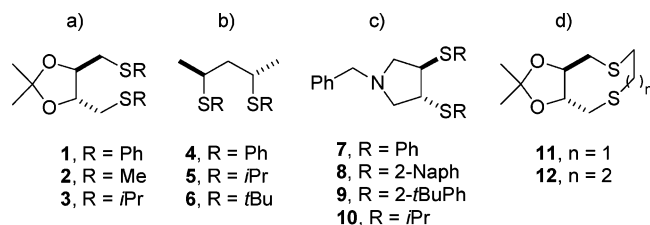
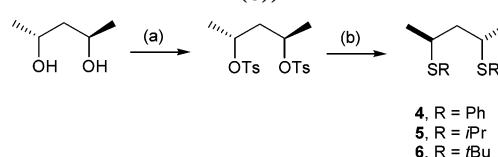


Figure 1. Chiral dithioethers: (a) type-DIOS (**1–3**); (b) type-DMPS (**4–6**); (c) type-DEGUS (**7–10**); and (d) type-DIOS-S (**11, 12**).

tivities.⁷ On the other hand, non- C_2 -symmetric dithioether derived from pyrrolidine also gave excellent enantioselectivities (up to 90%),^{8,9} but C_2 -symmetric S,S-homodonator dithioethers derived from 2,3-diisopropylidene treitol did not (enantioselectivities up to 42%).^{8a}

To rationalize these results, more examples were studied in which systematic changes of chelate ring size and electronic and steric effects of the sulfur substituents were performed. For these systems, it is also important to prepare intermediates and analyze the number of diastereomeric species formed in solution in order to understand the enantioinduction mechanisms. In this study we prepared chiral dithioethers type-DIOS (**1–3**), type-DMPS (**4–6**), and type-DEGUS (**7–10**) (Figure 1) and the corresponding palladium complexes with seven- to five-membered chelates. Sulfur inversion, which is often regarded as a cause of enantioselectivity erosion, can be effectively eradicated¹⁰ using bicyclic ligands such as type-DIOS-S (**11, 12**, Figure 1d), which forms butterfly metallabicycles with 7/5- and 7/6-members.⁸ Whenever possible, we studied the behavior of the solution and the solid-state structure in relation to the results obtained in catalytic studies in the allylic alkylation of *rac*-3-acetoxy-1,3-diphenyl-1-propene (*rac*-**I**) and *rac*-3-acetoxy-1-cyclohexene (*rac*-**III**) using dimethyl malonate as nucleophile. We also studied the regioselectivity of these systems using the terminal

Scheme 2. Synthesis of Type-DMPS Ligands: (a) See Ref 14; (b) NaH/RSH (R = Ph (4**), *i*Pr (**5**), *t*Bu (**6**))**



acetates (*E*)-3-acetoxy-1-phenyl-1-propene (**V**) and (*E/Z*)-1-acetoxy-2-butene (**VII**).

Results and Discussion

Synthesis of Ligands. Type-DIOS (**1–3**),¹¹ -DEGUS (**7** and **10**),¹² and -DIOS-S (**11, 12**)¹³ ligands were prepared as described in the literature (Figure 1). While this manuscript was being prepared, ligand **8** was synthesized using a different procedure.⁷ Ligands **8** and **9** were obtained by our previously described method from L-tartaric acid.¹² Ligands **4–6** were also synthesized by a two-step procedure (Scheme 2). The corresponding ditosylate was formed from the commercially available (2*R*,4*R*)-2,4-pentanediol.¹⁴ Further substitution of the tosylate by the phenylthiol group to form **4** proceeded at room temperature using THF as a solvent. It was necessary to heat up to 90 °C in DMF to obtain dithioethers **5** and **6**. The ligands were obtained as colorless oils in good yields (ca. 50–60%) and characterized by the usual techniques (see Experimental Section).

Pd-Catalyzed Allylic Alkylation. Allylic alkylation of the racemic 3-acetoxy substrates, *rac*-3-acetoxy-1,3-diphenyl-1-propene (*rac*-**I**) and *rac*-3-acetoxy-1-cyclohexene (*rac*-**III**), and terminal acetoxy derivatives, (*E*)-3-acetoxy-1-phenyl-1-propene (**V**) and (*E/Z*)-1-acetoxy-2-butene (**VII**) with dimethyl malonate as nucleophile, was carried out using Pd catalytic systems prepared in situ by adding the **1–12** ligands to the allylic dimer complex, [PdCl(C₃H₅)₂]. The results are shown in Tables 1–4.

The Pd-chiral dithioether **1–12** systems were tested as catalysts in the allylic alkylation of *rac*-**I** (Table 1). Our preliminary work in the allylic alkylation of *rac*-**I** with Pd/**1–12** catalyst precursors showed that the metallacycle size and the nature of the sulfur atom substituent (electronic induction and steric hindrance) influence the activity, but also the selectivity of the process.^{8a} Pd/type-DIOS systems afforded low conversions (entries 1–3, Table 1). The Pd/**1** system was not active (entry 1, Table 1) probably because **1** did not coordinate strongly enough to the metal.^{8b} When six- (ligands **4–6**) and five-membered (ligands **7–10**) metallacycles are involved, both aryl and alkyl S-substituted ligands were active. The DMPS systems showed higher activities than DEGUS systems (entries 4–6 vs 7–9, Table 1), except for the Pd/**10** catalytic system, which was as active as DMPS derivatives (entry 10 vs entries

(4) (a) Helmchen, G.; Pfaltz, A. *Acc. Chem. Res.* **2000**, *33*, 336. (b) Cozzi, P. G.; Zimmermann, N.; Hilgraf, R.; Schaffner, S.; Pfaltz, A. *Adv. Synth. Catal.* **2001**, *343*, 450. (c) Franco, D.; Gómez, M.; Jiménez, F.; Müller, G.; Rocamora, M.; Maestro, M. A.; Mahía, J. *Organometallics* **2004**, *23*, 3197.

(5) (a) Dawson, G. J.; Frost, C. G.; Martin, C. J.; Williams, J. M. J.; Coote, S. J. *Tetrahedron Lett.* **1993**, *34*, 7793. (b) Frost, C. G.; Williams, J. M. J. *Tetrahedron: Asymmetry* **1993**, *4*, 1785. (c) Frost, C. G.; Christopher, G.; Williams, J. M. J. *Tetrahedron Lett.* **1993**, *34*, 2015. (d) Togni, A. *Angew. Chem., Int. Ed. Engl.* **1996**, *35*, 1475. (e) Boog-Wick, K.; Pregosin, P. S.; Trabesinger, G. *Organometallics* **1998**, *17*, 3254. (f) You, S.-L.; Zhou, Y.-G.; Hou, X.-L.; Dai, L.-X. *Chem. Commun.* **1998**, 2765. (g) Koning, B.; Meetsma, A.; Kellogg, R. M. *J. Org. Chem.* **1998**, *63*, 5533. (h) Adams, H.; Anderson, J. C.; Cubbon, R.; James, D. S.; Mathias, J. P. *J. Org. Chem.* **1999**, *64*, 8256. (i) Chelucci, G.; Culeddu, N.; Saba, A.; Valentini, R. *Tetrahedron: Asymmetry* **1999**, *10*, 3537. (j) Fu, G. C. *Acc. Chem. Res.* **2000**, *33*, 412. (k) Rassias, G. A.; Page, P. C. B.; Reigier, S.; Christie, S. D. R. *Synlett* **2000**, 379–381. (l) You, S.-L.; Hou, X.-L.; Dai, L.-X.; Yu, Y.-H.; Xia, W. *J. Org. Chem.* **2002**, *67*, 4684. (m) Gómez, M.; Jansat, S.; Müller, G.; Maestro, M. A.; Mahía, J. *Organometallics* **2002**, *21*, 1077.

(6) Masdeu-Bultó, A. M.; Diéguez, M.; Martín, E.; Gómez, M. *Coord. Chem. Rev.* **2003**, *242*, 159.

(7) Khair, N.; Araújo, C. S.; Alvarez, E.; Fernández, I. *Tetrahedron Lett.* **2003**, *44*, 3401.

(8) (a) Jansat, S.; Gómez, M.; Müller, G.; Diéguez, M.; Aghmiz, A.; Claver, C.; Masdeu-Bultó, A. M.; Flores-Santos, L.; Martín, E.; Maestro, M. A.; Mahía, J. *Tetrahedron: Asymmetry* **2001**, *12*, 1469. (b) Flores-Santos, L.; Martín, E.; Aghmiz, A.; Diéguez, M.; Claver, C.; Masdeu-Bultó, A. M.; Muñoz Hernández, M. A. *Eur. J. Inorg. Chem.* **2005**, in press.

(9) Siedlecka, R.; Wojaczyńska, E.; Skarx0ewski, J. *Tetrahedron: Asymmetry* **2004**, *15*, 1437.

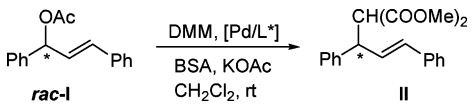
(10) Orrell, K. G. *Coord. Chem. Rev.* **1989**, *96*, 1.

(11) Diéguez, M.; Orejón, A.; Masdeu-Bultó, A. M.; Echarri, R.; Castellón, S.; Claver, C.; Ruiz, A. *J. Chem. Soc., Dalton Trans.* **1997**, 4611.

(12) Diéguez, M.; Ruiz, A.; Claver, C.; Pereira, M. M.; D'A. Rocha Gonsalves, A. M.; *J. Chem. Soc., Dalton Trans.* **1998**, 3517.

(13) Flores-Santos, L.; Martín, E.; Diéguez, M.; Masdeu-Bultó, A. M.; Claver, C. *Tetrahedron: Asymmetry* **2001**, *12*, 3029.


(14) Bakos, J.; Tóth, I.; Heil, B.; Markó, L. *J. Organomet. Chem.* **1981**, *279*, 23.

Table 1. Results of Asymmetric Allylic Alkylation of *rac*-I with Dimethyl Malonate (DMM) Catalyzed by [PdCl(C₃H₅)₂]/1–12^a


entry	ligand	time (h)	conv (%) ^b	ee II (%) ^c	ref
1	1	168	0		8a
2	2	168	95	8 (<i>R</i>)	this work
3	3	168	74	27 (<i>R</i>)	8a
4	4	60	100	26 (<i>R</i>)	this work
5	5	60	93	56 (<i>R</i>)	this work
6	6	60	95	70 (<i>R</i>)	this work
7	7	168	100	81 (<i>S</i>)	8a
8	8	144	80	76 (<i>S</i>)	this work
9	9	168	56	76 (<i>S</i>)	this work
10	10	60	100	30 (<i>S</i>)	8a
11	11	24	100	13 (<i>S</i>)	8a
12	12	24	100	42 (<i>S</i>)	8a

^a Catalytic conditions: catalytic precursor generated in situ from [PdCl(C₃H₅)₂] and the appropriated ligand (ratio Pd/L = 1/1.25); 1 mmol of *rac*-I, 3 mmol of DMM, 3 mmol of BSA, and a catalytic amount of KOAc in 4 mL of CH₂Cl₂ at room temperature.

^b Conversion based on the substrate. ^c Enantiomeric excesses determined by HPLC. Absolute configuration, in parentheses, determined by optical rotation: U. Leutenegger, G. Umbricht, C. Fahrni, P. V. Matt, A. Pfaltz, *Tetrahedron* **1992**, *48*, 2143–2156.

Table 2. Results of Asymmetric Allylic Alkylation of *rac*-III with Dimethyl Malonate (DMM) Catalyzed by [PdCl(C₃H₅)₂]/4–12^a


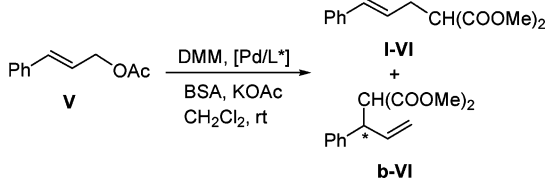
entry	ligand (%)	conv ^b (%)	ee IV ^c
13	4	72	27 (<i>R</i>)
14	5	98	21 (<i>R</i>)
15	6	93	20 (<i>R</i>)
16	7	3	n.d.
17 ^d	8	0	
18 ^d	9	3	n.d.
19	10	85	20 (<i>S</i>)
20	11	61	34 (<i>S</i>)
21	12	80	23 (<i>S</i>)

^a Catalytic conditions: catalytic precursor generated in situ from [PdCl(C₃H₅)₂] and the appropriate ligand (ratio Pd/L = 1/1.25); 1 mmol of *rac*-III, 3 mmol of DMM, 3 mmol of BSA, and a catalytic amount of KOAc in 4 mL of CH₂Cl₂ at room temperature.

^b Conversion based on the substrate. ^c Enantiomeric excesses determined by GC. Absolute configuration, in parentheses, determined by optical rotation: L. Xiao; W. Weissensteiner; K. Mereiter; M. Widhalm, *J. Org. Chem.* **2002**, *67*, 2206–2214. ^d The systems remain inactive after one week (reaction monitored by GC).

4–6, Table 1). These trends indicate that the most active palladium systems are those that contain five- and six-membered chelates and/or electrodonating groups on the sulfur atom.

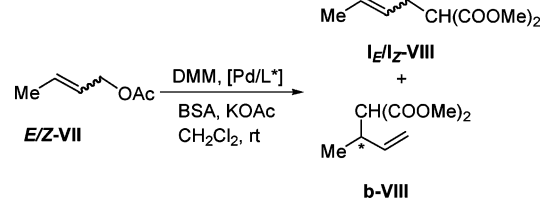
With regard to selectivity, very low asymmetric induction was observed with Pd/DIOS systems (entries 2 and 3, Table 1) (ee up to 27%). The best results were achieved with DEGUS ligands, with ee up to 81% (*S*) for **II** (entries 7–9, Table 1), but enantiomeric excess was also good with DMPS systems (up to 70% (*R*), entry 6, Table 1). For these DMPS systems, which contain a less strained metallic cycle (six-membered), asymmetric induction was enhanced when the steric hindrance of the S-substituent increased (entries 4–6, Table 1).

Table 3. Results of Asymmetric Allylic Alkylation of **V with Dimethyl Malonate (DMM) Catalyzed by [PdCl(C₃H₅)₂]/4–7,9–12^a**


entry	ligand	time (h)	conv (%) ^b	I/b-VI ^c
22	4	96	11	9/1
23	5	24	97	4/1
24	6	24	40	5/1 [75(<i>R</i>)] ^d
25	7	96	7	n.d.
26	9	72	0	
27	10	24	95	5/1 [37(<i>S</i>)] ^d
28	11	0.75	98	>9/1
29	12	0.75	98	>9/1

^a Catalytic conditions: catalytic precursor generated in situ from [PdCl(C₃H₅)₂] and the appropriated ligand (ratio Pd/L = 1/1.25); 1 mmol of **V**, 3 mmol of DMM, 3 mmol of BSA, and a catalytic amount of KOAc in 4 mL of CH₂Cl₂ at room temperature.

^b Conversion based on the substrate determined by ¹H NMR. ^c Ratio I/b-VI determined by GC. ^d In brackets, ee for **b-VI** determined by HPLC; absolute configuration, in parentheses, determined by optical rotation: L. Xiao; W. Weissensteiner; K. Mereiter; M. Widhalm, *J. Org. Chem.* **2002**, *67*, 2206.

Table 4. Results of Asymmetric Allylic Alkylation of **VII with Dimethyl Malonate (DMM) Catalyzed by [PdCl(C₃H₅)₂]/4,6–10,12^a**


entry	ligand	time (h)	conv (%) ^b	I _E /I _Z /b (VIII) ^b	I/b (VIII) ^c
30	4	16	61	75/n.d./25	3/1
31	6	24	81	35/3/62	1/1.6 [>99 (+)]
32	7	48	5	n.d.	n.d.
33	8	36	2	n.d.	n.d.
34	9	36	2	n.d.	n.d.
35 ^d	10	24	77	73/7/20	4/1
36	12	48	78	67/6/27	2.7/1

^a Catalytic conditions: catalytic precursor generated in situ from [PdCl(C₃H₅)₂] and the appropriate ligand (ratio Pd/L = 1/1.25); 1 mmol of **VII**, 3 mmol of DMM, 3 mmol of BSA, and a catalytic amount of KOAc in 4 mL of CH₂Cl₂ at room temperature.

^b Conversion based on the substrate determined by GC. ^c I/b = I_E + I_Z/b; in brackets, ee for **b-VIII** determined by HPLC. ^d After 48h, complete conversion of substrate was observed.

We designed bicyclic chiral ligands (*butterfly*-type) (**11**, **12**, Figure 1) in order to control the configuration of the sulfur stereocenters and consequently to decrease the number of diastereomers. The Pd precursors with the bicyclic ligands **11** and **12** induced moderate selectivity (ee up to 42% (*S*), entry 12 in Table 1), although they were significantly better than those obtained with type-DIOS ligands (entries 11 and 12 vs 2 and 3, Table 1). The *butterfly* systems were the most active, achieving complete conversion of the substrate after 24 h (entries 11 and 12, Table 1). This means that ligands **11** and **12**

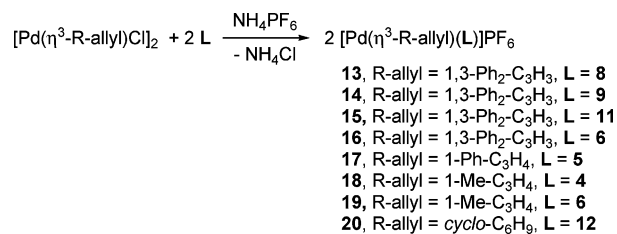
stabilize palladium species, which are more active than those formed by type-DIOS, -DMPS, and -DEGUS ligands, probably due to the simultaneous formation of two metallacycles (seven/five-membered rings for **11** and seven/six-membered rings for **12**).

We studied the Pd-catalyzed allylic alkylation of *rac*-**III** for DMPS, DEGUS, and DIOS-S ligands (Table 2). The catalytic reactions were quenched after 72 h. As observed for the noncyclic substrate *rac*-**I**, the Pd/DMPS systems (entries 13–15, Table 2) were more active than the Pd/DEGUS systems (entries 16–18, Table 2) except for Pd/**10**, whose activity was similar to Pd/DMPS derivatives (entry 19 vs 13–15). In fact Pd/**7–9** are inactive at the conditions studied. Pd systems with the bicyclic ligands, **11** and **12**, were also very active and the most enantioselective ones, achieving an ee up to 34% (*S*) for **IV**. The lower asymmetric induction in the alkylation of *rac*-**III** compared to the alkylation of *rac*-**I** (see Tables 1 and 2) was possibly due to the lower steric hindrance between the allyl and the bidentate ligand moieties in the palladium(II) intermediates.

The regioselectivity of the allylic alkylation reaction catalyzed with these chiral dithioethers was studied using substrate **V** (Table 3). TypePd/DIOS-S systems were highly active (total conversion of substrate in less than 1 h) and the most selective systems toward the linear isomer, **I-VI** (entries 28 and 29, Table 3). This behavior could be explained because the nucleophile attack on the less substituted terminal allyl carbon is sterically favored. However for DMPS and DEGUS systems a strong dependence on activity of the nature of the S-substituent was observed: while isopropyl substituents afforded practically total conversion of **V** in 24 h (entries 23 and 27, Table 3), aryl derivatives showed low activity (entries 22, 25, and 26, Table 3). Concerning the selectivity of DMPS and DEGUS systems, they also favor the formation of the linear product, but the ratio **I/b-VI** was minor compared with type-DIOS-S ligands, getting up to a 4/1 ratio (entries 23, 24, and 27, Table 3). The best enantiomeric excess for **b-VI** (75% (*R*)) was obtained with the DMPS-*t*Bu system (entry 24, Table 3). The relatively higher selectivity toward the branched product observed for Pd systems with ligands **5**, **6**, and **10** (entries 23, 24, and 27, Table 3) can be justified by the increase of electrophilicity of the terminal allylic carbon in the corresponding intermediate, due to the steric repulsion between the isopropyl or *tert*-butyl groups and the phenyl-substituted allyl carbon. The structural data of palladium intermediate complexes support this hypothesis (see below, Pd allylic complexes).

To enhance the electrophilic character of the substituted terminal allylic carbon, substrate **VII**, in which the phenyl allylic group is replaced by a methyl, was investigated (Table 4). As observed for substrate **V**, the most active systems were the Pd/**6** and Pd/**10** (entries 31 and 35, Table 4). All the active systems (entries 30, 31 and 35, 36, Table 4) showed a greater preference for the branched isomer than when phenyl substrate **V** was used. The highest regioselectivity in the branched isomer **b-VIII** was obtained with **6** (**b/l** = 1.6/1). In this case the enantioselectivity was very high and the branched isomer was obtained with a ee of >99% (entry 31, Table 4). This is a very remarkable result since it

Scheme 3. Synthesis of Allylic Complexes 13–20



clearly shows the efficiency of the ligand design. The **I/b-VIII** ratio is in agreement with the diastereomeric excess of the corresponding allyl complex, 1.3/1 (see below, NMR discussion for complex **19**).

Palladium Allylic Intermediates. To determinate the palladium allylic species formed with these ligands, we prepared allylic cationic complexes **13–20** following the method described previously (Scheme 3).¹⁵ These compounds were obtained as monometallic complexes of general formula [Pd(η³-R-allyl)(L)]PF₆ (R-allyl = 1,3-Ph₂-C₃H₃; 1-Ph-C₃H₄; 1-Me-C₃H₄; *cyclo*-C₆H₉), where L acts as a κ²-S,S-bidentate ligand.

These complexes were fully characterized by the usual techniques. Positive FAB mass spectra exhibited the peak at highest *m/z* ratio for the corresponding [Pd(η³-R-allyl)(L)]⁺ fragment. Structural studies were carried out both in the solid state (by X-ray diffraction on monocystal) and in solution (by NMR experiments).

Solid Structure of Complexes. Suitable crystals for X-ray determination were obtained for complexes **16–18** and **20**. Crystallographic data are listed in Table 5, and the ORTEP representations of the corresponding cations are given in Figures 2–5. In all cases the palladium(II) central atom presented a distorted square-planar environment with the corresponding π-allylic ligand and the dithioether coordinated as a chelate. The Pd–S and P–C allylic bond distances were in good agreement with π-allyl Pd(II) complexes containing dithioether^{8a} or S,X-donor ligands (S = thioether; X = N, P)^{3b,c,g,5h,m,16} reported in the literature.

For complex **16** two isomers were observed (**16a** and **16b**). The main difference between the two was in the relative disposition of the phenyl rings. The orientation of the allylic group was *exo* (*exo* is defined as the central C–H allylic bond pointing toward the same direction as the methylenic carbon atom of ligand **6** (–CH₂–)). No other diastereomers were found in the crystal structure. The six-membered chelate ring adopted a twist boat conformation in which the sulfur substituents were located in pseudoequatorial and pseudoaxial positions in a *SS* absolute configuration of the new sulfur stereocenters (total absolute configuration was *S*_C*S*_C–*S*_S*S*_S). In the two structures observed (**16a,b**), the allylic fragment was rotated with respect to the coordination S–Pd–S plane such that the two terminal C allylic atoms (C7 and C9 in **16a** or C46 and C48 in **16b**) lay in different sites of the S–Pd–S plane. This arrangement minimizes the repulsions between the aryl fragment and the equatorial substituent at the sulfur atom. The distances between the C allylic atoms and the nearly square plane formed by the Pd and the two sulfur atoms

(15) von Matt, P.; Lloyd-Jones, G. C.; Minidis, A. B. E.; Pfaltz, A.; Macko, L.; Neuburger, M.; Zehnder, M.; Rügger, H.; Pregosin, P. S. *Helv. Chim. Acta* **1995**, *78*, 265.

Table 5. Crystallographic Data for Complexes 16–18 and 20

	16	17	18	20
empirical formula	C ₂₈ H ₄₁ F ₄ PPdS ₂	C ₂₀ H ₃₃ F ₆ PPdS ₂	C ₂₁ H ₂₄ F ₆ PPdS ₂	C ₁₅ H ₂₅ F ₆ O ₂ PPdS ₂
fw	655.10	588.95	591.89	552.84
temp (K)	120(2)	298(2)	173(2)	298(2)
wavelength	0.71073	0.71073	0.71073	0.71073
cryst syst	monoclinic	monoclinic	orthorhombic	orthorhombic
space group	<i>P</i> 2 ₁	<i>P</i> 2 ₁	<i>P</i> 2 ₁ 2 ₁ 2 ₁	<i>P</i> 2 ₁ 2 ₁ 2 ₁
<i>a</i> (Å)	9.269(2)	9.0031(6)	11.1119(5)	9.5981(7)
<i>b</i> (Å)	15.385(4)	15.2391(11)	14.2590(7)	14.5774(10)
<i>c</i> (Å)	21.676(5)	19.1690(14)	15.4267(7)	15.4186(11)
β (deg)	99.615(4)	93.6840(10)		
volume (Å ³)	3047.7(12)	2624.5(3)	2444.3(2)	2157.3(3)
<i>Z</i>	4	4	4	4
ρ _{calcd} (g mL ⁻¹)	1.428	1.491	1.608	1.702
absorp coeff (mm ⁻¹)	0.838	0.974	1.047	1.186
<i>F</i> (000)	1352	1200	1188	1112
cryst size (mm ³)	0.63 × 0.36 × 0.06	0.29 × 0.23 × 0.19	0.44 × 0.41 × 0.25	0.50 × 0.10 × 0.10
θ range (deg)	1.63 to 28.35	2.13 to 28.27	1.94 to 26.38	1.92 to 26.00
index ranges	−12 ≤ <i>h</i> ≤ 12 −19 ≤ <i>k</i> ≤ 20 0 ≤ <i>l</i> ≤ 28	−5 ≤ <i>h</i> ≤ 11 −19 ≤ <i>k</i> ≤ 19 −24 ≤ <i>l</i> ≤ 23	−12 ≤ <i>h</i> ≤ 13 −17 ≤ <i>k</i> ≤ 17 −19 ≤ <i>l</i> ≤ 13	−11 ≤ <i>h</i> ≤ 10 −17 ≤ <i>k</i> ≤ 17 −19 ≤ <i>l</i> ≤ 18
no. of reflns collected	14 077	16 854	14 209	12 982
no. of indep reflns	14 077 [<i>R</i> (int) = 0.0000]	11 697 [<i>R</i> (int) = 0.0197]	4979 [<i>R</i> (int) = 0.0180]	4219 [<i>R</i> (int) = 0.0420]
absorp corr	none	semiempirical	semiempirical	semiempirical
no. of data/restraints/params	14 077/57/648	11 697/1/472	4979/0/318	4219/0/244
goodness-of-fit on <i>F</i> ²	1.039	1.026	1.038	1.019
final <i>R</i> indices [<i>I</i> > 2σ(<i>I</i>)] ^a	<i>R</i> 1 = 0.0644, w <i>R</i> 2 = 0.1655 ^b	<i>R</i> 1 = 0.0602, w <i>R</i> 2 = 0.1739 ^c	<i>R</i> 1 = 0.0488, w <i>R</i> 2 = 0.1245 ^d	<i>R</i> 1 = 0.0329, w <i>R</i> 2 = 0.0777 ^e
<i>R</i> indices (all data) ^a	<i>R</i> 1 = 0.0815, w <i>R</i> 2 = 0.1763 ^b	<i>R</i> 1 = 0.0718, w <i>R</i> 2 = 0.1852 ^c	<i>R</i> 1 = 0.0540, w <i>R</i> 2 = 0.1293 ^d	<i>R</i> 1 = 0.0396, w <i>R</i> 2 = 0.0803 ^e
absolute struct param ^f	0.00(4)	0.00	0.05(5)	−0.02(3)
largest diff peak and hole (e Å ⁻³)	1.396 and −1.507	1.013 and −1.118	1.058 and −0.812	0.494 and −0.537

^a *R*1 = Σ||*F*_o − |*F*_c|| and w*R*2 = {Σ[w(*F*_o² − *F*_c²)]/Σ[w(*F*_o²)]^{1/2}. ^b The weighting scheme employed was *w* = [σ²(*F*_o² + (0.0646*P*)² + 12.8603*P*)⁻¹ and *P* = (|*F*_o|² + 2|*F*_c|²)/3. ^c The weighting scheme employed was *w* = [σ²(*F*_o² + (0.1261*P*)² + 1.3861*P*)⁻¹ and *P* = (|*F*_o|² + 2|*F*_c|²)/3. ^d The weighting scheme employed was *w* = [σ²(*F*_o² + (0.0577*P*)² + 4.7963*P*)⁻¹ and *P* = (|*F*_o|² + 2|*F*_c|²)/3. ^e The weighting scheme employed was *w* = [σ²(*F*_o² + (0.0517*P*)² + 0.0000*P*)⁻¹ and *P* = (|*F*_o|² + 2|*F*_c|²)/3. ^f Flack, H. D. *Acta Crystallogr.* **1983**, *A39*, 876–881.

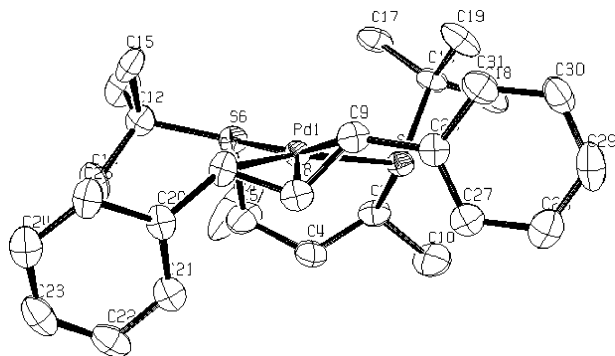


Figure 2. ORTEP view of the molecular structure of **16a**. Hydrogen atoms and hexafluorophosphate anions have been omitted for clarity. Selected bond distances (Å) and angles (deg) with esd's in parentheses: Pd(1)–C(7) = 2.196(7); Pd(1)–C(9) = 2.214(8); Pd(1)–S(6) = 2.360(2); Pd(1)–S(2) = 2.397(2); C(7)–Pd(1)–C(9) = 65.9(3); S(6)–Pd(1)–S(2) = 88.77(7).

show that the allylic ligand was rotated (Figure 6). A similar rotation of the allylic fragment was observed for S,*P*-donor ligands with ferrocenyl backbone (distances reported +0.004(3), +0.30(3), +0.85(3) Å),^{3b} but it has never been reported before for homodonor thioether ligands.

There were a number of differences between complexes **16** and **17**. In **17** the allylic fragment showed an *endo* disposition and the six-membered chelate ring adopted a chair conformation. The sulfur substituents were in equatorial and axial dispositions with a *S*_C–*S*_C*R*_S*R*_S absolute configuration. The *endo* orientation in

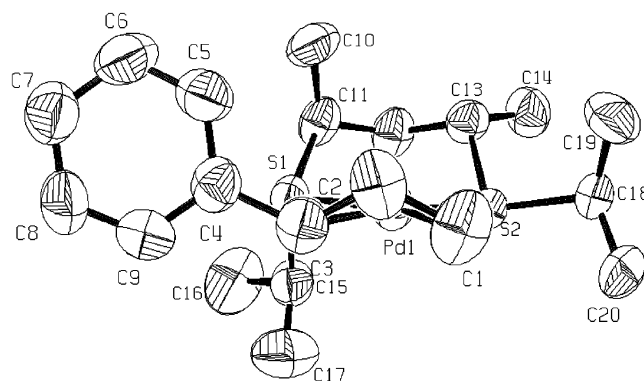


Figure 3. ORTEP view of the molecular structure of **17**. Hydrogen atoms and hexafluorophosphate anions are omitted for clarity. Selected bond distances (Å) and angles (deg) with esd's in parentheses: Pd(1)–C(1) = 2.166(10); Pd(1)–C(3) = 2.215(9); Pd(1)–S(1) = 2.3669(18); Pd(1)–S(2) = 2.345(2); C(1)–Pd(1)–C(3) = 67.6(4); S(2)–Pd(1)–S(1) = 92.61(6).

17 located the phenyl allylic moiety *cis* to the sulfur atom, which had the thioether isopropyl substituent in the *axial* position as in **16**, thus lowering the repulsion. The Pd–C distance *cis* to the S with the axial substituent was also longer than the Pd–C *trans*. Only one diastereomer was observed in solid state for complex **17**.

The structure of **18** showed a disorder in the central C allylic atom and in the methynic group of the dithioether ligand that correlated with a mixture of diastereomers **18a** (defined as *exo*) and **18b** (defined as

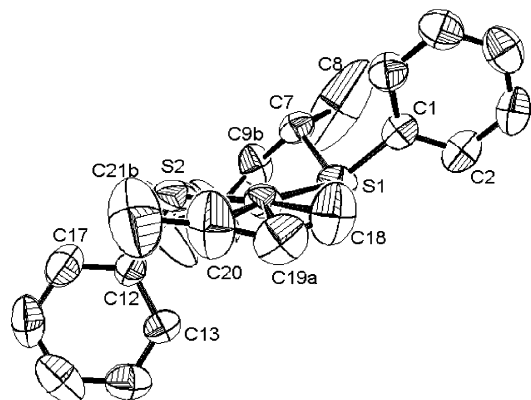


Figure 4. ORTEP view of the molecular structure of **18a**. Hydrogen atoms and hexafluorophosphate anions are omitted for clarity. Selected bond distances (Å) and angles (deg) with esd's in parentheses: Pd(1)–C(18) = 2.110(8); Pd(1)–C(20) = 2.177(9); Pd(1)–S(1) = 2.3536(18); Pd(1)–S(2) = 2.3436(18); C(18)–Pd(1)–C(20) = 68.1(4); S(2)–Pd(1)–S(1) = 94.86(8).

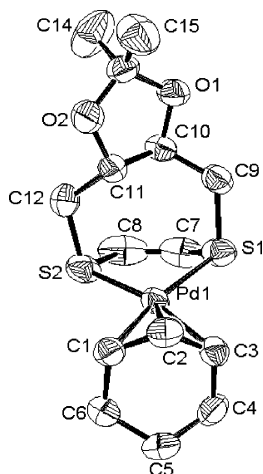


Figure 5. ORTEP view of the molecular structure of **20**. Hydrogen atoms and hexafluorophosphate anions are omitted for clarity. Selected bond distances (Å) and angles (deg) with esd's in parentheses: Pd(1)–C(1) = 2.139(4); Pd(1)–C(3) = 2.169(4); Pd(1)–S(1) = 2.3534(11); Pd(1)–S(2) = 2.3559(13); C(1)–Pd(1)–C(3) = 66.71(17); S(1)–Pd(1)–S(2) = 87.88(5).

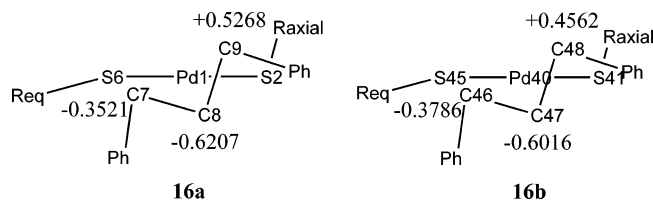


Figure 6. Distances (Å) of the C allylic atoms to the plane formed by the Pd and the two sulfur atoms.

endo) in a 65/35 ratio. In both cases the six-membered chelate ring had a twisted chair structure with different conformation and the two sulfur substituents in a relative *anti* orientation in pseudoequatorial/pseudoequatorial positions with $S_C S_C S_S S_S$ absolute configuration.

In complex **20**, the orientation of the allylic fragment was *exo* (relative to the central C–H allylic bond pointing in the same direction as the dioxolane ring). The other fragment of the cyclohexenyl ligand lies in the same region of the coordination plane as the five-

membered ring. The coordinated sulfur atoms had an *RS* absolute configuration, which was determined by the bicyclic structure of the ligand. Only one isomer was observed in solid state (see NMR discussion below). Palladium coordination to the dithioether ligand led to an envelope conformation of the five-membered ring and a twisted chair conformation for the seven-membered ring with the isopropylidene fragment. The η^3 -cyclohexenyl ligand was coordinated in such a way that the bulkier cyclic part was located on the opposite side of the isopropylidene moiety of the dithioether ligand in order to minimize repulsion.

Structural Studies in Solution. We performed NMR experiments for substituted allyl palladium complexes, **13**–**20** (Scheme 1), since they are key intermediates in the allylic alkylation reactions studied (^1H and ^{13}C NMR selected data are collected in Table S1, Supporting Information). When several isomers are formed, we expect the asymmetric induction to be low if the nucleophile reacts with them at a similar rate. These isomers are able to form due to (i) allyl relative disposition (the substituted allyl group can occupy *syn* or *anti* positions); (ii) diastereomers due to the stereogenic sulfur atoms; (iii) metallacycle conformation (boat and chair; as observed for the structures studied in the solid state, both of these are possible); and (iv) *exo* and *endo* isomers, according to the relative position of the allyl and metallacycle. Only *syn* allyl isomers were observed for the analyzed compounds in the studied temperature range.

Pd allylic complexes **13** and **14**, coordinated to DE-GUS ligands **8** and **9**, respectively, show the presence of four diastereomeric species (at 223 K, relative ratio for **13**, 10/10/10/1; at 243 K, for **14**, 4/3/2/1), which exhibited a fluxional behavior in solution. Results were similar for the Pd 1,3-diphenyl allyl derivative containing ligand **7**.^{8a} This isomeric distribution was in agreement with the two possible absolute configurations at the sulfur atom and the allylic arrangements relative to the ligand backbone (*exo*, *endo*), assuming free rotation for the N–CH₂Ph bond. Other Pd complexes containing DEGUS-type ligands provide additional evidence for a S,S-coordination in solution.¹⁷

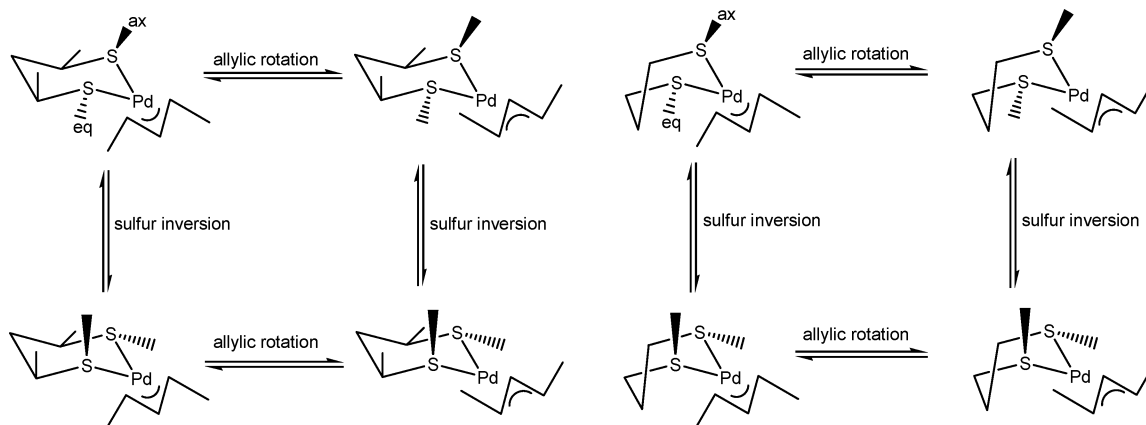
Complexes containing type-DMPS ligands (**16**–**19**) can form several isomers. Concerning the absolute configuration at the sulfur atoms, as observed in the analysis by X-ray diffraction (see above), these species adopt the same relative configuration, *R* or *S*, in the same complex. These facts decrease the number of isomers in solution, but up to eight isomers would be possible for symmetric disubstituted allyl groups and 16 for monosubstituted ones (Scheme 4).

VT ^1H NMR experiments were carried out (temperature range studied, 323–193 K). Two isomers were observed for complexes containing monosubstituted allyl groups, **17** (1-phenyl allyl), **18** (1-methyl allyl), and **19** (1-methyl allyl), whose ratio (ca. 1.3/1 for **17**; 1/1 for **18**; 1.3/1 for **19**) was practically invariable in the temper-

(16) (a) Herrmann, J.; Pregosin, P. S.; Salzmann, R.; Albinati, A. *Organometallics* **1995**, *14*, 3311. (b) Barbaro, P.; Currao, A.; Herrmann, J.; Nesper, R.; Pregosin, P. S.; Salzmann, R. *Organometallics* **1996**, *15*, 1879. (c) Enders, D.; Peters, R.; Runsink, J.; Bats, J. W. *Org. Lett.* **1999**, *1*, 1863.

(17) Diéguez, M.; Ruiz, A.; Masdeu-Bultó, A. M.; Claver, C. *J. Chem. Soc., Dalton Trans.* **2000**, 4154.

Scheme 4. Plausible Palladium Disubstituted Allylic Isomers for Complexes Containing Type-DMPS Ligands, with Chair (left) and Boat (right; methyl substituents on the dithioether backbone were omitted for clarity) Conformations



ature range studied. On the other hand, complex **16** (1,3-diphenyl allyl) showed a fluxional behavior: one isomer with sharp signals in the 298–273 K range; below 263 K, broad signals were formed, and below 213 K, sharp signals appeared again for two isomers in a ratio of ca. 1/1 (Figure 7).

The inversion barrier corresponding to boat-chair conformations was sufficiently high,¹⁰ thus NMR dynamic behavior was not expected. Additionally, 2D NOESY spectra did not show NOE contacts between the allyl and ligand moieties. Therefore, the two species observed in solution for **16** were probably due to two isomers, *exo* and *endo*, for a specified metallacycle conformation (boat or chair) with ($S_C S_C S_S S_S$) absolute configuration on the stereocenters (determined by X-ray diffraction). Taking into account the reactivity observed

for the allylic alkylation of *rac*-**I** (Table 1), the nucleophile will preferentially attack the more electrophilic terminal allylic carbon. For both isomers, the allylic carbon with more steric hindrance will be the most electrophilic carbon, so the same enantiomer will be obtained (Scheme 5). This argument is in agreement with the high enantiomeric excess observed for the Pd/**6** system (85 (*R*)/15 (*S*), entry 6, Table 1). Therefore, when the *S*-substituted groups are less bulky (ligands **4** and **5**), the electrodifferentiation between terminal allylic carbon atoms is lower and the ee must decrease (entries 4 and 5 vs 6, Table 1).

For complexes **18** and **19**, which contain the 1-methyl allyl group, exchange signals between both isomers for the allylic protons were detected. However, no exchange signals were observed for **17**, which contains the 1-

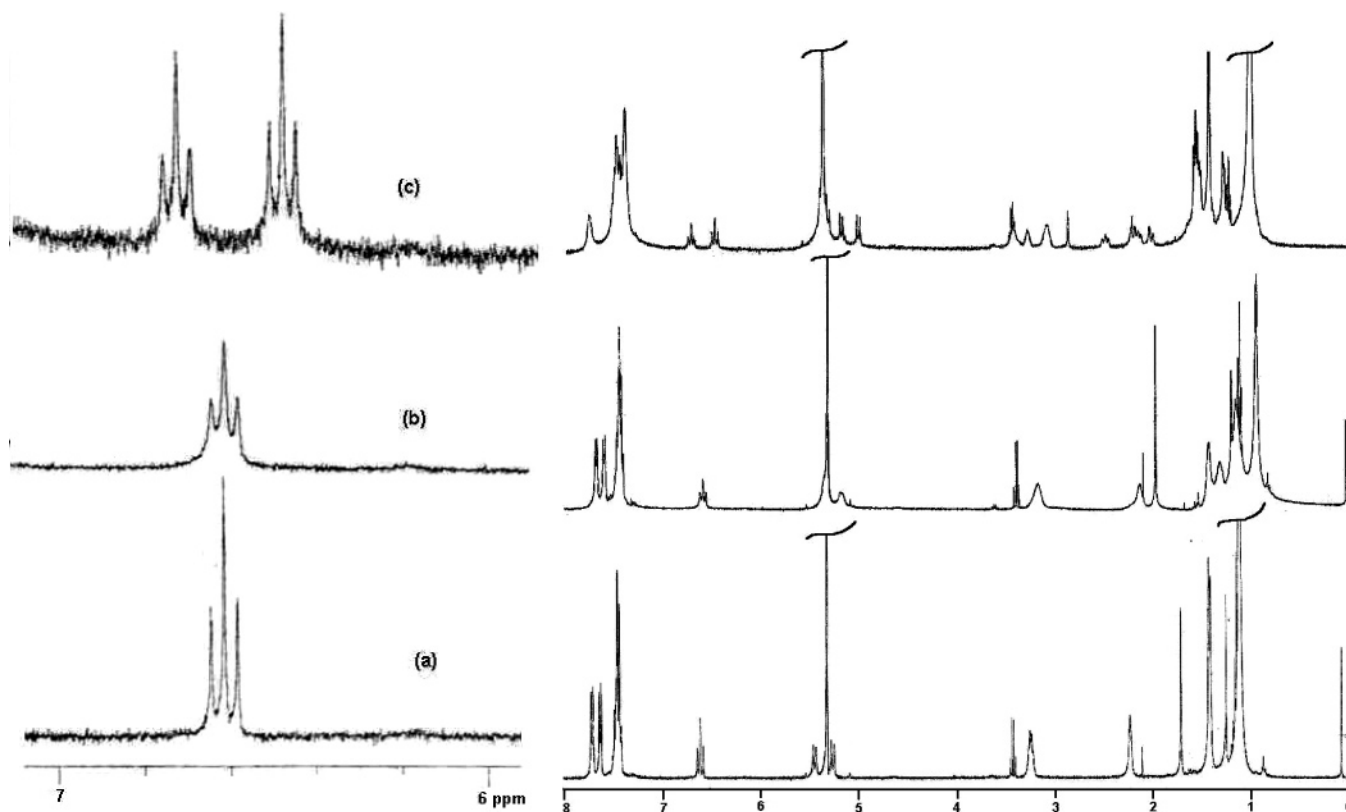
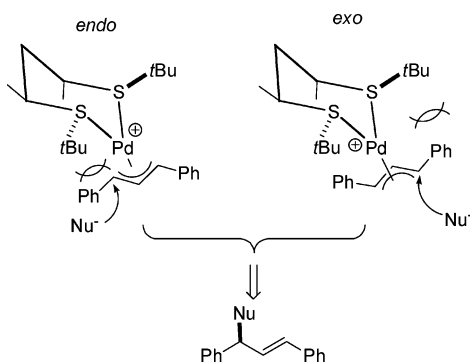


Figure 7. ^1H NMR (CD_2Cl_2 , 400 MHz) spectra for **16** (central allylic hydrogen region): (a) 298 K; (b) 253 K; (c) 193 K.

Scheme 5. Nucleophilic Attack on Palladium(II) Intermediates Containing the 1,3-Diphenyl Allyl and Ligand 6 (a chair metallacycle conformation is arbitrary chosen)



phenyl allyl group. The fact that the relative ratio of both isomers remains constant in the temperature range studied for the three complexes **17–19** indicates that the isomers may be due to different metallacycle conformations. In agreement with this behavior in solution, the X-ray diffraction study for **18** showed two metallacycle arrangements (see above).

For these complexes, the most important catalytic fact is the preference to afford the branched product in the case of **19**. Also, there was good agreement between the diastereomeric ratio of the two Pd isomers (1.3/1) and the regioselectivity of the process (**b/I-VIII** = 1.6/1, see Table 4). The difference in the ^{13}C chemical shift between both isomers for the terminal allyl carbon atoms was higher for **19** ($\Delta(\delta^{13}\text{C}) = 25$ (Isomer 1) and 35 (Isomer 2) ppm; see Table S1) than for **18** ($\Delta(\delta^{13}\text{C}) = 21$ (Isomer 1) and 23 (Isomer 2) ppm, see Table S1). The electrophilicity of the substituted allyl carbon for **19** was enhanced, so the branched product was afforded by the external nucleophilic attack.

Concerning the complexes coordinated to dithioether cyclic ligands, both complexes **15** and **20** showed only one species at room temperature. But two isomers, corresponding to *exo* and *endo* conformations, were distinguished at low temperature with a diastereomeric ratio ca. 4/1 in both cases. For *butterfly*-type ligands, disagreement between diastereomeric and enantiomeric excess was then produced, due to the low electronic differentiation between both terminal allylic carbon atoms ($\Delta(\delta^{13}\text{C}) = 1.7$ for **15** and 1.4 ppm for **20**; see Table S1) and lack of ligand hindrance around the allyl moiety, as observed in the X-ray diffraction structure determination of **20** (see above).

Conclusions

The systematic catalytic study carried out in this paper makes evident not only the significant activity of the new Pd/dithioether compounds in allylic alkylation reactions but the notable selectivity for symmetrical and nonsymmetrical allylic substrates. Concerning the catalytic activity, the *butterfly* dithioethers (**11**, **12**) show, for all four alkylations considered, high activities and excellent regioselectivity toward the linear product; in fact **I-VI** was obtained in roughly pure form from the alkylation of (*E*)-3-acetoxy-1-phenyl-1-propene (**V**). In relation to the selectivity toward the chiral alkylated

products, the systems containing type-DEGUS ligands give very good enantiomeric excesses for the alkylation of the model substrate *rac*-**I** (ee up to 81%). Furthermore, DMPS derivatives induce selectivity in the case of the less hindered allyl groups (*rac*-**III**) and the terminal acetoxy substrates (**V** and **VII**); thus, the branched isomer **b-VI** was obtained with an ee up to 75% and **b-VIII** was the major product in the alkylation of (*E/Z*)-1-acetoxy-2-butene (**VII**), with an excellent asymmetric induction (>99%).

The structural analysis of allylic palladium intermediates (**13–20**) by NMR spectroscopy allows the understanding of the catalytic behavior observed. The X-ray diffraction data indicate the coordination mode of the complexes, in particular the metallacycle type formed. With reference to *butterfly* ligands (**11**, **12**), the low enantioselectivity induced by these Pd systems is due to the insignificant electronic differentiation between both terminal allylic carbon atoms, as shown by their close ^{13}C chemical shift ($\Delta(\delta^{13}\text{C})$ less than 2 ppm) and their lack of ligand hindrance toward the allyl group, as observed in the solid state for complex **20**. Although complexes containing DEGUS ligands show several diastereomers in solution (**13**, **14**), very good enantioselectivity is observed for product **II**, especially when electron-withdrawing groups (**7–9**) are bonded to the sulfur atom. Consequently the interconversion among the isomers should be faster than the nucleophilic attack. But for complexes containing DMPS ligands (**16–19**), a good matching between diastereomeric ratio and selectivity toward the alkylated products is observed, in agreement with the constant diastereomeric composition in solution (VT NMR spectra). This means that the palladium isomers should react at the same rate with the nucleophile. In summary, the selectivity in the Pd-catalyzed allylic alkylation containing homodonor dithioether ligands can be controlled by the thermodynamics of the palladium diastereomer formation (high energy barrier between Pd isomers, as is the case for type-DMPS ligands) or by the kinetics of the nucleophilic attack (low energy barrier among the palladium species, as is the case for type-DEGUS ligands), depending on the nature of the metallacycle.

Experimental Section

General Data. All compounds were prepared under a purified nitrogen atmosphere using standard Schlenk and vacuum-line techniques. The solvents were purified by standard procedures and distilled under nitrogen. $[\text{Pd}(\eta^3\text{-C}_3\text{H}_5)(\mu\text{-Cl})_2]$,¹⁸ $[\text{Pd}(\eta^3\text{-1,3-Ph}_2\text{-C}_3\text{H}_3)(\mu\text{-Cl})_2]$,¹⁵ and ligands **1–3**,¹¹ **7–10**,¹² and **11** and **12**¹³ were prepared as previously described. (2*R*,4*R*)-2,4-Pentanediol was purchased from Aldrich and was used without further purification. NMR spectra were recorded on Varian XL-500, Bruker DRX 500, Varian Gemini 200, Bruker DRX 250, and Varian Unity Nova 300 spectrometers at 298 K in CDCl_3 unless otherwise cited. Chemical shifts were reported downfield from standards. FAB mass spectra were obtained on Fisons V6-Quattro and JEOL SX102A instruments using 3-nitrobenzyl alcohol as matrix. MALDI mass spectra were obtained on a VOYAGER-DE-RP instrument using 1,8,9-trihydroxiantracene as matrix. The GC analyses were performed on a Hewlett-Packard 5890 Series II gas chromatograph (50 m Ultra 2 capillary column 5% phenylmethylsilicone and 95% dimethylsilicone) with a FID detector. The GC/MS

analyses were performed on a Hewlett-Packard 5890 Series II gas chromatograph (50 m Ultra 2 capillary column) interfaced to a Hewlett-Packard 5971 mass selective detector. Optical rotations were measured on a Perkin-Elmer 241MC spectropolarimeter. Enantiomeric excesses were determined by HPLC on a Hewlett-Packard 1050 Series chromatograph (Chiralcel-OD and Chiralcel-OJ chiral columns) with a UV detector, and by GC on a Hewlett-Packard 5890 Series II gas chromatograph (25 m FS-cyclodex- β -I/P column: heptakis-(2,3,6-tri-*O*-methyl)- β -cyclodextrin/polysiloxan) with a FID detector. Elemental analyses were carried out by the Serveis Científicotècnics of the University of Barcelona in an Eager 1108 microanalyzer.

The ligands **4–6**, **8**, and **9** were prepared from the chiral bis(trifluoromethylsufanyloxy)¹² or ditosyl¹⁴ derivatives and the appropriate thiol. One example is described below, and synthetic details for analogous compounds are given in the Supporting Information.

(2S,4S)-2,4-Bis(thiophenyl)pentane (4). A solution of phenylthiol (0.16 mL, 1.17 mmol) in THF (2 mL) was added to a suspension of 0.14 g of NaH (60%, 3.5 mmol) (in paraffin washed with hexane) in THF (2 mL). The mixture was stirred for 1 h at room temperature. After this time a solution of (2*R*,4*R*)-2,4-ditosylpentane¹⁴ (0.23 g, 0.56 mmol) in THF (2.5 mL) was added to the suspension. The reaction was followed by TLC (ethyl acetate/hexane = 1/3). After 5 h the solvent was evaporated and dichloromethane (5 mL) was added. The solution was cooled to 0 °C and carefully treated with water (5 mL). Phases were separated, and the aqueous phase was extracted with dichloromethane (3 × 3 mL). The organic phase was then dried and concentrated. The residue was purified by flash column chromatography with silica gel (ethyl acetate/hexane = 1/200). Compound **4** was obtained as a colorless oil (0.096 g, 60% yield). ¹H NMR (400 MHz): δ 1.29 (d, 6H, J = 6.4 Hz), 1.73 (t, 2H, J = 7.0 Hz), 3.52 (sext, 2H, J = 6.9 Hz), 7.2–7.3 (m, 6H), 7.4 (m, 4H). ¹³C{¹H} NMR (100.6 MHz): δ 22.23 (CH₃) 41.88 (CH₂), 43.91 (CH), 127.24 (C), 129.04 (C), 132.80 (C), 134.74 (C). Anal. Calcd for C₁₇H₂₀S₂: C 70.83, H 6.94, S 22.22. Found: C 70.33, H 7.40, S 21.46. $[\alpha]_D^{23}$ = -70.31° (c 0.63, CHCl₃). FAB⁺ MS: m/z 288.4 m/z [M]⁺ (calcd 288.1006 for C₁₇H₂₀S₂⁺).

(2S,4S)-2,4-Bis(thio-2-propyl)pentane (5): colorless oil (0.07 g, 57% yield). ¹H NMR (400 MHz): δ 1.2–1.3 (m, 18H), 1.58 (t, 2H, J_{H-H} = 6.6 Hz), 2.9–3.1 (m, 4H). ¹³C{¹H} NMR (100.6 MHz): δ 22.91 (CH₃), 24.06 (CH₃), 24.10 (CH₃), 33.98 (CH), 36.87 (CH₂), 45.25 (CH). $[\alpha]_D^{23}$ = -46.3° (0.80, CHCl₃). Anal. Calcd for C₁₁H₂₄S₂: C 59.93, H 10.97, S 29.09. Found: C 60.20, H 12.70, S 26.42. FAB⁺ MS: m/z 221.0 m/z [M + H]⁺ (calcd 221.1398 for C₁₁H₂₅S₂⁺).

(2S,4S)-2,4-Bis(thio-2-methylpropyl)pentane (6): colorless oil (0.08 g, 54% yield). ¹H NMR (400 MHz): δ 1.31 (d, 6H, J = 6.4 Hz), 1.34 (s, 18H), 1.61 (t, 2H, J = 7.2 Hz), 2.98 (sext, 2H, J = 6.8 Hz). ¹³C{¹H} NMR (100.6 MHz): δ 24.92 (CH₃), 32.24 (CH₃), 36.06 (CH), 43.44 (C), 47.97 (CH₂). $[\alpha]_D^{23}$ = -106° (0.8, CHCl₃). Anal. Calcd for C₁₃H₂₈S₂·0.1CH₂Cl₂: C 61.31, H 10.99, S 24.94. Found: C 60.85, H 11.35, S 24.45. FAB⁺ MS: m/z 250.1 m/z [M + 2H]⁺ (calcd 250.1789 for C₁₃H₃₀S₂⁺).

(3*R*,4*R*)-3,4-Bis(thio-2-naphthyl)-1-benzylpyrrolidine (8): white solid (0.31 g, 73% yield). Mp: 83–85 °C. ¹H NMR (300 MHz): δ 2.78 (m, 2H), 3.31 (m, 2H), 3.71 (AB, 2H, J = 12.9 Hz), 3.81 (m, 2H), 7.2–7.8 (m, 19H). ¹³C{¹H} NMR (75.5 MHz): δ 52.04 (CH), 59.15 (CH₂), 59.54 (CH₂), 126, 126.44, 127.12, 127.25, 127.63, 128.31, 128.42, 128.57, 128.68, 129.89, 132.07, 132.3 (CH), 133.51 (C), 138.24 (C). $[\alpha]_D^{25}$ = +101.27° (c 1.2, CHCl₃). FAB⁺ MS: m/z 478 m/z [M + 1H]⁺ (calcd 478.1663 for C₃₁H₂₈NS₂⁺). HR-FAB⁺ MS: 478.1654 m/z (Err[ppm/mmu] = -1.8/-0.9).

(3*R*,4*R*)-3,4-Bis(thio-2-*tert*-butylphenyl)-1-benzylpyrrolidine (9): colorless oil (0.32 g, 77% yield). ¹H NMR (300 MHz): δ 1.47 (s, 18H, C(CH₃)₃), 2.71 (dd, 2H, CHH–N, ² J = 9.6 Hz, ³ J = 4.5 Hz), 3.21 (dd, 2H, CHH–N, ³ J = 6.6 Hz), 3.74

(AB, 2H, CH_AH_BPh, J = 13.2 Hz), 3.8 (m, 2H, SCH), 6.9–7.4 (m, 13H, C₆H₄, C₆H₅). ¹³C{¹H} NMR (75.5 MHz): δ 30.6 (CH₃), 36.54 (CH₃), 52.98 (CH), 59.63 (CH₂), 59.71 (CH₂), 126.34, 126.41, 126.53, 127.04, 128.24, 128.61, 133.84 (CH), 135.01 (C), 138.27 (C), 144.88 (C). $[\alpha]_D^{25}$ = +42.58° (c 1.2, CHCl₃). FAB⁺ MS: m/z 490 m/z [M + 1H]⁺ (calcd 490.2602 for C₃₁H₄₀NS₂⁺). HR-FAB⁺ MS: 490.2615 m/z (Err[ppm/mmu] = +2.6/+1.3).

The complexes [Pd(η^3 -R-allyl)(L)]PF₆ **13–20** were prepared from [Pd(η^3 -R-allyl)Cl]₂, NH₄PF₆, and the appropriate chiral dithioethers ligand. One example is described below (see Supporting Information for synthetic details of all complexes).

[Pd(η^3 -1,3-Ph₂-C₃H₃)(8)]PF₆ (13). Ligand **8** (0.08 g, 0.167 mmol) and the complex of [Pd(μ -Cl)(η^3 -1,3-Ph₂-C₃H₃)]₂ (0.05 g, 0.075 mmol) were dissolved in a mixture of ethanol, chloroform, dichloromethane, and methanol (1:1:1:1, 30 mL) at room temperature under nitrogen. NH₄PF₆ (0.08 g, 0.491 mmol) was then added, and the mixture was stirred for 4 days. The mixture was then filtered, the solvent was removed under reduced pressure, and the remaining solid was dissolved in dichloromethane (15 mL). The organic phase was washed with water (3 × 10 mL), dried over Na₂SO₄, and filtered off, and the solvent was then evaporated to afford an orange solid. The product was recrystallized from a mixture of dichloromethane and diethyl ether (0.107 g, 72% yield). ¹H NMR (300 MHz): δ 2.1–3.2 (br m, 4H, CH₂N), 3.3–3.7 (br m, 2H), 3.8–4.4 (br m, 2H), 5.08–6.10 (br m, 2H), 6.5–8.2 (m, 30H). ¹³C{¹H} NMR (75.5 MHz): δ 51.98 (CH), 58.32 (CH₂), 59.37 (CH₂), 86–91 (CH), 107.29 (CH), 125.6–136.7 (C). ¹H NMR (300 MHz, 223 K, allylic zone): δ 6.51–6.72 (m, 1H); Isomer 1 (36%) δ 5.06 (d, 1H, J = 10.8 Hz), 5.44 (d, 1H, J = 12 Hz); Isomer 2 (34%) δ 5.38 (d, 1H, J = 12.3 Hz), 5.56 (d, 1H, J = 12 Hz); Isomer 3 (27%) δ 5.07 (d, 1H, J = 12 Hz), 5.96 (d, 1H, J = 12.9 Hz); Isomer 4 (3%) δ 5.48 (1H), 5.85 (d, 1H, J = 10.8 Hz). FAB⁺ MS: m/z 776 [M – PF₆]⁺ (calcd 776.1653 for C₄₆H₄₀NS₂Pd⁺). HR-FAB⁺ MS: m/z 776.1622, (Err[ppm/mmu] = -1.9/-1.5).

[Pd(η^3 -1,3-Ph₂-C₃H₃)(9)]PF₆ (14): orange solid (0.101 g, 71%). ¹H NMR (300 MHz, 293 K): δ 0.75, 0.9–1.2 (m, 18H), 2.2–3.4 (m, 6H), 3.5–4.6 (m, 2H), 4.82 (d, 0.4H, J = 11.4 Hz), 5–5.6 (m, 1.2H), 5.98 (d, 0.4H, 1H, J = 12.3 Hz), 6.1–8.2 (m, 24H). ¹³C{¹H} NMR (75.5 MHz): δ 29.55, 30.62 (CH₃), 36.26 (CH₃), 52.67 (CH), 58.47 (CH₂), 59.68 (CH₂), 86–91 (CH), 107.30 (CH), 116.53, 120.57, 126.62–136.83, 142.25–143.72 (C), 150.04 (C). ¹H NMR (300 MHz, 223 K, allylic zone): Isomer 1 (44%) δ 4.74 (d, 1H, J = 11.4 Hz), 5.92 (d, 1H, J = 12.3 Hz) 6.57 (pt, 1H); Isomer 2 (28%) δ 5.07 (d, 1H, J = 11.7 Hz), 5.43 (d, 1H, J = 11.4 Hz) 6.71 (pt, CH_{central}); Isomer 3 (22%) δ 5.01 (d, 1H, J = 11.4 Hz), 5.38 (d, 1H, J = 13.2 Hz) 6.06 (pt, 1H); Isomer 4 (6%) δ 5.29 (d, 1H, J = 10.8 Hz), 5.88 (d, 1H, J = 10.6 Hz). FAB⁺ MS: m/z 788 [M – PF₆]⁺ (calcd 788.2592 for C₄₆H₅₂NS₂Pd⁺). HR-FAB⁺ MS: m/z 788.2519 (Err[ppm/mmu] = -7.2/-5.7).

[Pd(η^3 -1,3-Ph₂-C₃H₃)(11)]PF₆ (15): yellow solid (0.043 g, 94% yield). ¹H NMR (300 MHz, 293 K): δ 1.37 (s, 6H) 2.04 (br m, 2H), 2.84, 3.01 (br m, 4H), 3.31 (br m, 2H) 4.09 (br m, 2H), 5.68 (d, 1H, J = 11.7 Hz), 5.74 (d, 1H, J = 12.3 Hz), 6.83 (pt, 1H, J = 12 Hz), 7.38–7.46 (m, 6H), 7.52–7.62 (m, 4H). ¹³C{¹H} NMR (75.5 MHz): δ 26.37 (CH₃), 32–41 (CH₂), 82.71 (CH), 87.14 (CH), 88.79 (CH), 108.88 (CH), 110.07 (C), 127.08, 127.16 (C), 129.38, 129.45 (C), 129.64 (C), 136.48, 136.61 (C). ¹H NMR (300 MHz, 243 K, allylic zone): Isomer 1 (78%) δ 5.66 (d, 1H, J = 12 Hz), 5.74 (d, 1H, J = 12.3 Hz), 6.86 (t, 1H, J = 12.3 Hz); Isomer 2 (22%) δ 5.51 (d, 1H, J = 11.7 Hz), 5.66 (d, 1H, J = 12 Hz), 6.78 (pt, 1H, J = 12 Hz). FAB⁺ MS: m/z 519 [M – PF₆]⁺ (calcd 519.0652 for C₂₄H₂₉O₂S₂Pd⁺). HR-FAB⁺ MS: m/z 519.0638 (Err[ppm/mmu] = -1.0/-0.5).

[Pd(η^3 -1,3-Ph₂-C₃H₃)(6)]PF₆ (16): orange solid (0.068 g, 75% yield). ¹H NMR (400 MHz, CD₂Cl₂): δ 1.11 (s, 18H), 1.42 (d, 6H, J = 6.8 Hz), 2.24 (br t, 2H), 3.24 (br sext, 2H, J = 6.0 Hz), 5.27 (d, 1H, J = 12.4 Hz), 5.46 (d, 1H, J = 12.8 Hz), 6.62 (t, 1H, J = 12.4 Hz), 7.45 (m, 6H), 7.63 (d, 2H, J = 6.8 Hz), 7.72 (d, 2H, J = 7.2 Hz). ¹³C{¹H} NMR (100.6 MHz, CD₂Cl₂):

δ 24.68 (CH₃), 30.76 (CH₃), 38.07 (CH), 49.20 (CH₂), 51.99 (C), 88.41 (CH), 90.73 (CH), 108.56 (CH), 129.74 (C), 129.96 (C), 130.29 (C), 137.28 (C). Anal. Calcd. for C₂₈H₄₁F₆PS₂Pd: C 48.54, H 5.92, S 9.23. Found: C 49.10, H 6.00, S 9.55. FAB⁺ MS: m/z 546.9 m/z [M - PF₆]⁺ (calcd 547.1685 for C₂₈H₄₁S₂-Pd⁺).

[Pd(η^3 -1-Ph-C₃H₄)(5)]PF₆ (**17**): yellow solid (0.132 mg, 66% yield). ¹H NMR (400 MHz, CD₂Cl₂): Isomer 1 (56%) δ 1.19 (d, 3H, J = 7.2 Hz), 1.22 (d, 3H, J_{H-H} = 6.8 Hz), 1.31 (d, 3H, J_{H-H} = 7.2 Hz), 1.39 (d, 3H, J = 6.8 Hz), 1.42 (d, 3H, J = 6.8 Hz), 1.49 (d, 3H, J = 6.8 Hz), 2.15 (m, 2H), 3.12 (psxt, 1H, J = 6.8 Hz), 3.20 (m, 1H), 3.35 (m, 1H), 3.45 (m, 1H), 3.46 (d, 1H, J = 12.4 Hz), 4.64 (d, 1H, J = 7.2 Hz), 4.98 (d, 1H, J = 12.4 Hz), 6.24 (dt, 1H, J_{H-H} = 12.4 Hz, 7.2 Hz), 7.45 (m, 3H), 7.50 (m, 2H); Isomer 2 (44%) δ 0.85 (d, 3H, J_{H-H} = 6.8 Hz), 1.06 (d, 3H, J = 6.4 Hz), 1.40 (d, 3H, J = 6.8 Hz), 1.46 (d, 3H, J = 6.4 Hz), 1.47 (d, 3H, J = 7.2 Hz), 2.20 (m, 2H), 2.84 (psxt, 1H, J = 6.8 Hz), 3.25 (m, 1H), 3.45 (m, 2H), 3.56 (d, 1H, J = 12.4 Hz), 4.55 (d, 1H, J = 7.2 Hz), 5.25 (d, 1H, J = 12.4 Hz), 6.26 (dt, 1H, J = 12.4 Hz, 7.2 Hz), 7.40 (m), 7.55 (m). ¹³C{¹H} NMR (100.6 MHz, CD₂Cl₂): Isomer 1 δ 20.71 (CH₃), 21.90 (CH₃), 22.14 (CH₃), 22.62 (CH₃), 23.07 (CH₃), 23.46 (CH₃), 37.10 (CH), 37.36, 39.86 (CH), 40.26 (CH), 41.04 (CH₂), 66.58 (CH₂), 92.21 (CH), 114.05 (CH), 129.89 (CH), 129.97 (CH), 130.14 (CH), 135.91 (C); Isomer 2 δ 21.80 (CH₃), 21.98 (CH₃), 22.08 (CH₃), 22.68 (CH₃), 22.92 (CH₃), 23.03 (CH₃), 37.18 (CH), 37.51 (CH), 40.19 (CH), 40.34 (CH), 42.06 (CH₂), 65.07 (CH₂), 93.94 (CH), 112.96 (CH), 128.74 (CH), 128.80 (CH), 135.07 (C). Anal. Calcd. for C₂₀H₃₃F₆PS₂Pd: C 40.79, H 5.65, S 10.89. Found: C 41.11, H 5.61, S 10.08. FAB⁺ MS: m/z 443.5 [M - PF₆]⁺ (calcd 443.1059 for C₂₀H₃₃S₂Pd⁺).

[Pd(η^3 -1-Me-C₃H₄)(4)]PF₆ (**18**): yellow solid (0.065 g, 55% yield). ¹H NMR (400 MHz, CD₂Cl₂): δ 1.25 (dd, 3H, Isomer 1, J = 6.4 Hz, 0.4 Hz), 1.19 (dd, 3H, Isomer 2, J_{H-H} = 6.4 Hz, 0.4 Hz), 1.28 (d, 3H, J = 6.8 Hz), 1.35 (d, 3H, J = 6.8 Hz), 1.39 (d, 3H, J = 7.2 Hz), 1.54 (d, 3H, J = 6.8 Hz), 2.12 (m, 1H), 2.17 (m, 2H), 2.25 (m, 1H), 3.03 (dt, 1H, J = 12.8 Hz, J = 1.2 Hz), Isomer 2 3.39 (dt, 1H, Isomer 1, J = 12.8 Hz, J = 1.2 Hz), 3.60 (m, 2H), 3.66 (dd, 1H, Isomer 1, J = 7.2 Hz, J = 1.2 Hz), 3.70 (m, 2H), 3.77 (dd, 1H, Isomer 2, J = 7.2 Hz, J = 1.2 Hz), 4.07 (psxt, 1H, Isomer 1, J = 6.4 Hz), 4.44 (psxt, 1H, Isomer 2, J = 6.4), 5.53 (m, 1H, Isomer 2), 5.64 (m, 1H, Isomer 1), 7.82 (m, 2H), 7.70 (m, 6H, CH), 7.55 (m, 12H, CH). ¹³C{¹H} NMR (100.6 MHz, CD₂Cl₂): δ 17.33 (CH₃, Isomer 1), 17.41 (CH₃, Isomer 2), 20.48 (CH₃), 20.97 (CH₃), 21.19 (CH₃), 21.67 (CH₃), 39.19 (CH₂), 39.33 (CH₂), 43.61 (CH₂), 44.26 (CH₂), 45.08 (CH₂), 70.55 (CH₂, Isomer 2), 71.51 (CH₂, Isomer 1), 92.28 (CH, Isomer 1), 93.21 (CH, Isomer 2), 121.19 (CH), 135–130.6 (CH + C). Anal. Calcd. for C₂₁H₂₇F₆PS₂Pd: C 42.39, H 4.57, S 10.78. Found: C 42.00, H 4.45, S 10.20. FAB⁺ MS: m/z 449.5 [M - PF₆]⁺ (calcd 449.0589 for C₂₁H₂₇S₂Pd⁺).

[Pd(η^3 -1-Me-C₃H₄)(6)]PF₆ (**19**): yellow solid (0.118 g, 70% yield). ¹H NMR (400 MHz, CDCl₃): δ Isomer 1 (56.5%): 1.25–1.73 (m, 27H), 1.95–2.31 (br s, 1H), 2.54–2.65 (m, 1H), 3.11–3.23 (br s, 1H), 3.32–3.45 (br s, 1H), 3.24 (d, J = 12.6 Hz, 1H), 4.15 (m, 1H), 4.52 (d, J = 7.0 Hz, 1H), 5.68 (m, 1H); Isomer 2 (43.5%): 1.25–1.73 (m, 27H), 1.95–2.31 (br s, 2H), 3.11–3.23 (br s, 1H), 3.52–3.60 (br s, 1H), 3.43 (d, J = 12.7 Hz, 1H), 4.28 (d, J = 7.7 Hz, 1H), 4.70 (m, 1H), 5.46 (m, 1H). ¹³C{¹H} NMR (100 MHz, CDCl₃): δ Isomer 1 18.07 (CH₃), 26.69 (C), 29.8–31.5 (8CH₃), 40.41 (C), 48.43 (CH₂), 66.10 (CH₂), 91.20 (CH), 118.85 (CH); Isomer 2 18.71 (CH₃), 22.06 (C), 29.8–31.5 (8CH₃), 33.83 (C), 48.87 (CH₂), 63.38 (CH₂), 98.00 (CH), 117.63 (CH). Anal. Calcd. for C₁₇H₃₅F₆PS₂Pd: C 36.79, H 6.36, S 11.55. Found: C 36.50, H 6.20, S 11.80. MALDI MS: m/z 409.10 [M - PF₆]⁺ (calcd 409.1215 for C₁₇H₃₅S₂Pd⁺).

[Pd(η^3 -cyclo-C₆H₉)(12)]PF₆ (**20**): yellow solid (0.105 g, 48% yield). ¹H NMR (500 MHz, 278 K): δ 1.02 (m, 1H, CH₂-CHHCH₂ cyclohexylallyl), 1.33, 1.39 (s, 6H, CH₃ Isomer 1 80%, Isomer 2 20%), 1.55 (m, 1H), 1.76 (m, 2H), 2.3 (m, 2H), 2.62 (m, 2H), 2.79, 3.07 (m, 4H), 3.39 (m, 2H) 4.05 (m, 2H), 5.74 (t,

1H, ³ J = 6.5 Hz), 6.01 (t, 1H, ³ J = 6.5 Hz), 6.07 (t, 1H, ³ J = 6.5 Hz). ¹³C{¹H} NMR (375 MHz, 278 K): δ 17.1 (CH₂), 26.6 (CH₃, Isomer 1), 27.3 (CH₃, Isomer 2), 29.6 (CH₂), 34.2 (CH₂), 35.3 (CH₂), 79.8 (CH), 87.5 (CH), 88.9 (CH), 111.25 (CH). FAB⁺ MS: m/z 407 [M - PF₆]⁺ (calcd 407.0331 for C₁₅H₂₅O₂S₂Pd⁺). HR-FAB⁺ MS: m/z 407.0328 (Err[ppm/mmu] = -0.7/-0.3).

General Procedure for Palladium-Catalyzed Allylic Alkylation. Allylic Alkylation of *rac*-3-Acetoxy-1,3-diphenyl-1-propene (I). The catalytic precursor was generated in situ from [Pd(η^3 -C₃H₅)(μ -Cl)]₂ and the appropriate ligand (0.02 mmol of Pd and 0.025 mmol of chiral ligand) in 2 mL of CH₂Cl₂ for 30 min before adding the substrate. *rac*-3-Acetoxy-1,3-diphenyl-1-propene (0.252 g, 1 mmol), dissolved in CH₂-Cl₂ (2 mL), was added followed by dimethyl malonate (0.396 g, 3 mmol), BSA (0.610 mg, 3 mmol), and a catalytic amount of KOAc. The mixture was stirred at room temperature until total conversion of the substrate (monitored by TLC, unless stated otherwise). The solution was then diluted with diethyl ether, filtered over Celite, and washed with saturated ammonium chloride solution (4 \times 10 mL) and water (4 \times 10 mL). The organic phase was dried over anhydrous Na₂SO₄ and filtered off, and the solvent was removed under reduced pressure. The product was purified by column chromatography (SiO₂; ethyl acetate). The enantiomeric excesses were determined by HPLC on a Chiralcel OD column, using hexane/2-propanol, 99/1, as eluent in a flow of 0.3 mL/min.

Allylic Alkylation of *rac*-3-Acetoxy-1-cyclohexene (III). The procedure was analogous to the one described for the *rac*-3-acetoxy-1,3-diphenyl-1-propene. The product was purified by column chromatography (SiO₂; ethyl acetate). The enantiomeric excesses were determined by GC on a FS-cyclodex- β -I/P column.

Allylic Alkylation of (*E*)-3-Acetoxy-1-phenyl-1-propene (V) and (*E/Z*)-1-Acetoxy-2-butene (VII). The procedure was analogous to the one described for the *rac*-3-acetoxy-1,3-diphenyl-1-propene. The product was purified by column chromatography (SiO₂; ethyl acetate). Regioselectivity was determined by GC, and the enantiomeric excesses for **b-VI** and **b-VIII** were determined by HPLC on a Chiralcel-OJ chiral column, using hexane/2-propanol as eluent: 87/13 in a flow of 0.7 mL/min for **b-VI** and 95/5 in a flow of 0.5 mL/min for **b-VIII**.

Crystallography. Suitable crystals for X-ray diffraction of **16–18** and **20** were obtained by slow diffusion of diethyl ether into a dichloromethane solution of the complex. Crystal data are shown in Table 5. The crystals were measured in a Bruker SMART CCD diffractometer, with a graphite-monochromated Mo K α radiation (λ = 0.71073 Å). Absorption corrections were applied using the SADABS program.¹⁹ The structures were solved by direct methods using the SHELXS-97 computer program²⁰ for crystal structure determination, except for **16**, which was solved by the DIRDIF96 program,²¹ and refined by full-matrix least-squares method on F^2 , with the SHELXL-97 computer program.²² Hydrogen atoms were included in calculated positions and refined in riding mode.

CCDC-224192 and -224193 (**16**), CCDC-224194 (**17**), CCDC-224195 (**18**), and CCDC-224196 (**20**) contain the supplementary crystallographic data for this paper. These data can be obtained free of charge at www.ccdc.cam.ac.uk/contents/retrieving.html (or from the Cambridge Crystallographic Data Cen-

(19) Sheldrick, G. M. *SADABS, A Program for Empirical Absorption Correction of Area Detector Data*; University of Göttingen: Germany, 1996. Based on the method of Robert Blessing; Blessing, R. H. *Acta Crystallogr.* **1995**, *A51*, 33.

(20) Sheldrick, G. M. *SHELXS 97*, a computer program for crystal structure determination; University of Göttingen, 1997.

(21) Beurskens, P. T.; Beurskens, G.; Bosman, W. P.; de Gelder, R.; Garcia-Granda, S.; Gould, R. O.; Israel, R.; Smits, J. M. M. *The DIRDIF96 Program System*, Technical Report of the Crystallography Laboratory; University of Nijmegen, 1996.

(22) Sheldrick, G. M. *SHELXL 97*, a computer program for crystal structure refinement; University of Göttingen, 1997.

tre, 12 Union Road, Cambridge CB21EZ, UK; fax: (+44) 1223-336-033; or deposit@ccdc.cam.ac.uk).

Acknowledgment. The authors would like to thank the Ministerio de Educación y Ciencia (CTQ2004-01546/BQU), DGAPA-UNAM (PAPIIT IN-202902-3), and the Generalitat de Catalunya for financial support. The installation of the SMART CCD single-crystal diffrac-

tometer at the University of A Coruña was supported by the Xunta de Galicia (XUGA INFRA-97).

Supporting Information Available: File containing additional information on synthetic procedures and Table S1, and CIF file for complexes **16–18** and **20**. This material is available free of charge via the Internet at <http://pubs.acs.org>.

OM050190S